

# Stability of gravity-driven free-surface flow past a deformable solid at zero and finite Reynolds number

Gaurav and V. Shankar<sup>a)</sup>

Department of Chemical Engineering, Indian Institute of Technology, Kanpur 208 016, India

(Received 30 June 2006; accepted 19 January 2007; published online 28 February 2007)

The linear stability of Newtonian liquid flow down an inclined plane lined with a deformable elastic solid layer is analyzed at zero and finite Reynolds number. There are two qualitatively different interfacial modes in this composite system: the free-surface or gas-liquid (“GL”) mode which becomes unstable at low wave numbers and nonzero Reynolds number in flow down a rigid plane, and the liquid-solid (“LS”) mode which could become unstable even in the absence of inertia at finite wave numbers when the solid layer is deformable. The objectives of this work are to examine the effect of solid layer deformability on the GL and LS modes at zero and finite inertia, and to critically assess prior predictions concerning GL mode instability suppression at finite inertia obtained using the linear elastic model by comparison with the more rigorous neo-Hookean model for the solid. In the creeping-flow limit where the GL mode instability is absent in a rigid incline, we show that for both solid models, the GL and LS modes become unstable at finite wavelengths when the solid layer becomes sufficiently soft. At finite wavelengths, the labeling of the two interfacial modes as GL and LS becomes arbitrary because these two modes get “switched” when the solid layer becomes sufficiently deformable. The critical strain required for instability becomes independent of the solid thickness (at high enough values of thickness) for both GL and LS modes in the linear elastic solid, while it decreases with the thickness of the neo-Hookean solid. At finite Reynolds number, it is shown for both the solid models that the free-surface instability in flow down a rigid plane can be suppressed at all wavelengths by the deformability of the solid layer. The neutral curves associated with this instability suppression are identical for both linear elastic and neo-Hookean models. When the solid becomes even more deformable, both the GL and LS modes become unstable for finite wave numbers at nonzero inertia, but the corresponding neutral curves obtained from the two solid models differ significantly in detail. At finite inertia, for both the solid models, there is a significant window in the shear modulus of the solid for moderate values of solid thickness where both the GL and LS modes are stable at all wave numbers. Thus, using the neo-Hookean model, the present study reaffirms the prediction that soft elastomeric coatings offer a passive route to suppress and control interfacial instabilities. © 2007 American Institute of Physics. [DOI: 10.1063/1.2698582]

## I. INTRODUCTION

Free-surface and two-layer flows are well known to exhibit interfacial instabilities due to viscosity contrasts (in Newtonian liquids)<sup>1–4</sup> and elasticity contrasts (in viscoelastic liquids).<sup>5,6</sup> From a technological standpoint (e.g., film coating operations), there is considerable interest in the manipulation and suppression of these interfacial instabilities by various means. Previous studies<sup>7–10</sup> have suggested “active” methods such as imposed wall oscillations or heating as possible strategies for suppressing interfacial instabilities. Recently, the possibility of using deformable solid coatings as a “passive” method to suppress interfacial instabilities in two-layer and free-surface flows was explored for both Newtonian<sup>11,12</sup> and viscoelastic<sup>13,14</sup> fluids. These studies, however, employed the linear elastic model<sup>15</sup> to describe the deformation in the solid, which is valid only when the deformation gradients in the solid are small. In a recent paper,

Gkanis and Kumar<sup>16</sup> used the more rigorous neo-Hookean model<sup>17,18</sup> and demonstrated in the creeping-flow limit that the predictions from the two solid models could be significantly different for the stability of flow down an inclined plane covered with a deformable solid, and noted that the earlier predictions of instability suppression<sup>11,12</sup> must be re-examined using the neo-Hookean solid model. The free-surface instability is absent in the creeping-flow limit, so it is necessary to consider nonzero Reynolds number in order to analyze the suppression of free-surface instability by the deformable solid. To this end, we undertake here a comprehensive study of stability of liquid flow down an inclined plane lined with a deformable solid, at zero and finite Reynolds number. The primary objective of the present work is to critically evaluate earlier predictions<sup>11,12</sup> concerning instability suppression obtained using the linear elastic model by comparing them with the results from the neo-Hookean solid model. Before proceeding, we briefly discuss related previous work in order to place our work in a proper context.

Yih<sup>1</sup> (also see Refs. 3, 4, 19, and 20) used a long-wave

<sup>a)</sup> Author to whom correspondence should be addressed. Electronic mail: vshankar@iitk.ac.in

analysis to show that the free surface [referred to hereafter as the GL (gas-liquid) mode] in liquid flow down an inclined plane becomes unstable at sufficiently low (but nonzero) Reynolds number. For small angles of inclination, falling films on inclined planes display both free-surface and shear instability modes.<sup>21</sup> The presence of another liquid layer in the case of two-layer flow down an inclined plane leads to interaction of the two interfaces in the system, and renders the flow unstable<sup>22–25</sup> even at zero Reynolds number. In the two-layer configuration considered in the present work, the liquid adjacent to the inclined rigid surface is replaced by a deformable solid layer, and the consequence of the interaction between the liquid-solid interface and the free surface is analyzed here both at zero and finite Reynolds number. When a viscous liquid flows past a deformable solid surface, the stresses exerted by the fluid at the fluid-solid interface cause deformation in the solid layer, which could alter the adjacent fluid flow. Kumaran *et al.*<sup>26</sup> (also see Refs. 27–29) considered the stability of plane Couette flow of a Newtonian fluid past a linear viscoelastic solid, and showed that the liquid-solid interface becomes unstable beyond a critical strain even in the creeping-flow regime. We refer to this instability as the liquid-solid (LS) interfacial mode. Clearly, this mode will be present even when there is more than one liquid layer adjacent to the solid. For two-layer or free-surface flow past a deformable solid, it was shown using the linear viscoelastic solid model<sup>11,12</sup> that the deformability of the solid could lead to complete suppression of the interfacial instabilities under appropriate conditions, without destabilizing the LS mode. Specifically, Shankar and Sahu<sup>12</sup> considered the stability of liquid flow down an inclined plane lined with a linear viscoelastic solid layer at finite Reynolds number, and showed that beyond a critical value of a solid deformability parameter (which is proportional to the ratio of viscous forces in the liquid to elastic forces in the solid), the inertia-driven GL mode instability can be suppressed at all wave numbers. When the solid deformability parameter is further increased, this has a destabilizing effect on both the GL and LS modes, which become unstable at *finite* wave numbers.

However, Gkanis and Kumar<sup>27,30</sup> pointed out that at finite deformations, appropriate modifications must be made to the linear elastic model in order to obey the principle of material-frame indifference.<sup>15,18</sup> They instead used the neo-Hookean model, which is a rigorous generalization of the Hookean elastic solid to finite deformations, in order to analyze the stability of plane Couette flow past a deformable surface. Importantly, the neo-Hookean solid yields a first-normal stress difference in the base state, and the discontinuity of this normal stress in the base state at the liquid-solid interface was shown to give rise to a short-wave instability. For solid to fluid thickness ratio smaller than 1, the short-wave mode significantly modifies the critical conditions for instability. More recently, Gkanis and Kumar<sup>16</sup> studied the same configuration as in Ref. 12, but used the neo-Hookean model to describe the solid deformation, and considered the creeping-flow limit where the GL mode instability is absent in rigid surfaces. Their results showed that the solid deformability destabilizes only one of the two interfacial modes,

which they identified as the LS mode (in the present nomenclature). They further concluded that the GL mode is not destabilized by the solid deformability, for both the solid models. This result is at variance with the predictions of Shankar and Sahu.<sup>12</sup> Another important conclusion reached by Gkanis and Kumar<sup>16</sup> is that the critical nondimensional strain for the finite-wave number instability becomes independent of the solid thickness for the linear elastic model, while it decreases with thickness for the neo-Hookean model. In view of these qualitative differences in results from the two solid models, the question arises as to whether the earlier predictions of instability suppression<sup>11,12</sup> obtained using the linear elastic model will remain true for the more rigorous neo-Hookean solid model. To answer this question, we revisit the problem of stability of flow down an inclined plane lined with a deformable solid modeled using both linear elastic and neo-Hookean models, at both zero and finite Reynolds number. In what follows, the formulation of the problem is briefly outlined in Sec. II. The solution methodology used to obtain the different unstable modes is described in Sec. III A, while the results at the zero-Re limit and the finite-Re case are discussed, respectively, in Sec. III B and Sec. III C. We end with the main conclusions of this study in Sec. IV.

## II. PROBLEM FORMULATION

The system under consideration (see Ref. 12 for a schematic figure) is comprised of an incompressible Newtonian liquid flowing past an incompressible and impermeable deformable solid. The solid (of density  $\rho$ , thickness  $HR$ , and shear modulus  $E$ ) is strongly bonded to a rigid inclined plane at  $z^* = (1+H)R$  which makes an angle  $\theta$  with the horizontal. The liquid layer (of viscosity  $\mu$  and density  $\rho$ ) is in contact with a passive gas and occupies a region  $0 \leq z^* \leq R$ . The densities of liquid and solid are assumed to be equal without loss of generality. Various physical quantities are nondimensionalized at the outset by using the following scales:  $R$  for lengths and displacements, free-surface velocity of liquid layer in the base-state  $V = \rho g R^2 \sin \theta / 2\mu$  for velocities and  $\mu V / R$  for stresses and pressure. (Reference 12 uses the average velocity in the liquid as the velocity scale, while we use here the maximum velocity.) The deformation in the solid layer is described by the linear elastic model as well as the neo-Hookean model. In the interests of brevity, we omit the presentation of the governing equations in the fluid and the linear viscoelastic solid, and these can be found in the earlier works.<sup>12,16</sup>

It suffices here to mention that the governing equations for the fluid are written in terms of spatial ( $\mathbf{x} = x, y, z$ ) coordinates, while it is convenient (following Gkanis and Kumar<sup>27</sup>) to refer to the governing equations for the solid in terms of a reference configuration, where the independent variables are the spatial positions  $\mathbf{X} = (X, Y, Z)$  of material particles in the reference (i.e., unstressed) configuration. Thus, the spatial ( $x, y, z$ ) coordinate system used for fluid motion is identical to the reference ( $X, Y, Z$ ) coordinate system for the deformable solid. In the deformed state of the solid, the spatial positions of the material particle are de-

noted in this study by  $\mathbf{w}(\mathbf{X})=(w_X, w_Y, w_Z)$ , and this is equivalent to a Lagrangian description<sup>15</sup> of motion in the solid. The displacement vector of material points is given by  $\mathbf{u}(\mathbf{X}) \equiv \mathbf{w}(\mathbf{X}) - \mathbf{X}$ . The parameter  $\Gamma = \mu V / ER$  that occurs in the governing equations of the solid is the nondimensional solid deformability parameter and can be interpreted as the estimated ratio of viscous shear stresses in liquid to elastic stresses in the solid layer. When  $\Gamma \rightarrow 0$ , we obtain the limit of a rigid solid layer. The previous studies of Gkanis and Kumar<sup>27,30,16</sup> have employed the neo-Hookean model in the absence of inertial effects in the solid. In the present study, it is important to include inertial effects in the liquid in order to capture the free-surface instability. Since the densities of the fluid and the deformable solid layer are usually comparable, it is therefore necessary to include inertial effects in the solid layer as well. The mass and momentum conservation equations governing the dynamics of an incompressible neo-Hookean solid with inertia are:<sup>15,18</sup>

$$\det(\mathbf{F}) = 1, \quad (1)$$

$$\text{Re} \left[ \frac{\partial^2 \mathbf{w}}{\partial t^2} \right]_{\mathbf{X}} = \nabla_{\mathbf{X}} \cdot \mathbf{P} + \frac{2}{\sin \theta} \hat{\mathbf{g}}. \quad (2)$$

The inertial forces (per unit volume) in the left-hand side of Eq. (2) is simply the density of the solid multiplied by the acceleration of a material particle, which, in the reference description, is given by  $\left[ \partial^2 \mathbf{w} / \partial t^2 \right]_{\mathbf{X}}$  (see, e.g., Holzapfel<sup>18</sup>, pp. 62 and 145). Here,  $\mathbf{P}$  is the first Piola-Kirchhoff tensor and  $\mathbf{F} = \nabla_{\mathbf{X}} \mathbf{w}$  is the deformation gradient tensor. The first Piola-Kirchhoff stress tensor is related to Cauchy stress tensor by  $\mathbf{P} = \mathbf{F}^{-1} \cdot \boldsymbol{\sigma}$ , where the Cauchy stress tensor for the neo-Hookean solid is given by<sup>17,18</sup>

$$\boldsymbol{\sigma} = -\hat{p}_s \mathbf{I} + \frac{1}{\Gamma} (\mathbf{F} \cdot \mathbf{F}^T), \quad (3)$$

where  $\hat{p}_s$  is the pressure-like function related to actual pressure  $p_s$  in the neo-Hookean solid as  $\hat{p}_s = p_s + 1/\Gamma$ .

The laminar base state of the present system consists of unidirectional flow of liquid in the  $x$  direction due to gravity. The solid layer is at rest in this steady state with a nonzero displacement in the  $x$  direction due to liquid shear stress at the interface. Both GL and LS interfaces remains flat in the base state. The base-state velocity and displacement fields are identical to those given in Refs. 12 and 16 except for the difference in the scheme of nondimensionalization. The linearized equations governing the stability of the composite system are obtained in a manner similar to the one described in Refs. 12 and 16, and are presented here for the sake of completeness. In the ensuing analysis,  $k$  is the wave number of fluctuations,  $c$  is the complex wavespeed, and  $\tilde{v}_z$  is the eigenfunction for the  $z$  component of fluid velocity perturbation; similarly,  $\tilde{u}_Z$  is the eigenfunction for the  $z$  component of the solid displacement perturbation. The linearized equations for the liquid layer are

$$\frac{d\tilde{v}_z}{dz} + ik\tilde{v}_x = 0, \quad (4)$$

$$\text{Re}[ik(\tilde{v}_x - c)\tilde{v}_x + (d_z \tilde{v}_x)\tilde{v}_z] = -ik\tilde{p} + \left[ \frac{d^2}{dz^2} - k^2 \right] \tilde{v}_x, \quad (5)$$

$$\text{Re}[ik(\tilde{v}_x - c)\tilde{v}_z] = -\frac{d\tilde{p}}{dz} + \left[ \frac{d^2}{dz^2} - k^2 \right] \tilde{v}_z. \quad (6)$$

The governing equations for the linear elastic solid are

$$\frac{d\tilde{u}_Z}{dZ} + ik\tilde{u}_X = 0, \quad (7)$$

$$-\text{Re} k^2 c^2 \tilde{u}_X = -ik\tilde{p}_s + \frac{1}{\Gamma} \left[ \frac{d^2}{dZ^2} - k^2 \right] \tilde{u}_X, \quad (8)$$

$$-\text{Re} k^2 c^2 \tilde{u}_Z = -\frac{d\tilde{p}_s}{dZ} + \frac{1}{\Gamma} \left[ \frac{d^2}{dZ^2} - k^2 \right] \tilde{u}_Z, \quad (9)$$

and for the neo-Hookean model

$$\frac{d\tilde{w}_Z}{dZ} + ik\tilde{w}_X + \underline{(2\Gamma Z)ik\tilde{w}_Z} = 0, \quad (10)$$

$$-ik\tilde{p}_s + \underline{(2 \cot \theta)ik\tilde{w}_Z} + \frac{1}{\Gamma} \left[ -k^2 + \frac{d^2}{dZ^2} \right] \tilde{w}_X = -k^2 c^2 \text{Re} \tilde{w}_X, \quad (11)$$

$$\underline{-(2\Gamma Z)ik\tilde{p}_s} - \underline{(2 \cot \theta)ik\tilde{w}_X} - \frac{d\tilde{p}_s}{dZ} + \frac{1}{\Gamma} \left[ -k^2 + \frac{d^2}{dZ^2} \right] \tilde{w}_Z = -k^2 c^2 \text{Re} \tilde{w}_Z. \quad (12)$$

The terms underlined in Eqs. (10)–(12) and in the interfacial condition (22) (see below) represent the additional couplings between base state and perturbation quantities that occur for the neo-Hookean solid and are absent for the linear elastic solid.<sup>16,27</sup> The linearized kinematic and boundary conditions at the unperturbed free surface ( $z=0$ ) are

$$ik[\tilde{v}_x(z=0) - c]\tilde{h} = \tilde{v}_z(z=0), \quad (13)$$

$$-2\tilde{h} + \left( \frac{d\tilde{v}_x}{dz} + ik\tilde{v}_z \right) = 0, \quad (14)$$

$$-\tilde{p} - (2 \cot \theta)\tilde{h} + 2\frac{d\tilde{v}_z}{dz} - k^2 \Sigma \tilde{h} = 0. \quad (15)$$

Here,  $\Sigma = \gamma / \mu V$  is the nondimensional interfacial tension parameter (which is the inverse of the capillary number), with  $\gamma$  as the dimensional GL interfacial tension. Similarly, the linearized boundary conditions at the LS interface ( $z=1$ ) for the linear elastic solid are:

$$\tilde{v}_z = -ikc\tilde{u}_Z, \quad (16)$$

$$\tilde{v}_x + \tilde{u}_Z(d_z \tilde{v}_x)_{z=1} = -ikc\tilde{u}_X, \quad (17)$$

$$\frac{d\tilde{v}_x}{dz} + ik\tilde{v}_z = \frac{1}{\Gamma} \left( \frac{d\tilde{u}_x}{dZ} + ik\tilde{u}_z \right), \quad (18)$$

$$-\tilde{p} + 2\frac{d\tilde{v}_z}{dz} + k^2\Sigma_1\tilde{u}_z = -\tilde{p}_s + \frac{2}{\Gamma} \frac{d\tilde{u}_z}{dZ}, \quad (19)$$

and for the neo-Hookean solid are:

$$\tilde{v}_z = -ikc\tilde{w}_z, \quad (20)$$

$$\tilde{v}_x + \tilde{w}_z(d_z\tilde{v}_x)_{z=1} = -ikc\tilde{w}_x, \quad (21)$$

$$(-4\Gamma^2)ik\tilde{w}_z - (2\Gamma)\frac{d\tilde{w}_z}{dZ} + ik\tilde{w}_z + \frac{d\tilde{w}_x}{dZ} = \Gamma \left( \frac{d\tilde{v}_x}{dz} + ik\tilde{v}_z \right), \quad (22)$$

$$-\tilde{p} + 2\frac{d\tilde{v}_z}{dz} + \tilde{p}_s - \frac{2}{\Gamma} \frac{d\tilde{w}_z}{dZ} + k^2\Sigma_1\tilde{w}_z = 0. \quad (23)$$

Here,  $\Sigma_1 = \gamma_1/\mu V$  is the nondimensional LS interfacial tension parameter, with  $\gamma_1$  as the dimensional LS interfacial tension. Finally, the boundary conditions at the rigid surface ( $z=1+H$ ) are  $\tilde{\mathbf{u}}=0$ , for the linear elastic solid and  $\tilde{\mathbf{w}}=0$ , for the neo-Hookean solid.

### III. RESULTS

#### A. Solution methodology and mode identification

In this section, we explain how we identify and label the two different interfacial modes (GL and LS) present in the system. For the linear elastic solid at  $\text{Re}=0$ , the stability problem is solved analytically,<sup>26</sup> and the characteristic equation is cubic in the complex wavespeed  $c$  at  $\text{Re}=0$ . In the previous low- $k$  asymptotic analysis,<sup>12</sup> it was shown that the leading order wavespeed (a real quantity) for GL mode in flow past a deformable solid is equal to the leading order wavespeed for the GL mode obtained by Yih<sup>1</sup> for rigid surfaces. With the deformable solid layer, at  $\text{Re}=0$ , the real part of one of the three roots approaches the leading order wavespeed of the low- $k$  asymptotic solution<sup>1,12</sup> for small  $k$ . The magnitude of the imaginary part of this root tends to zero as  $k \rightarrow 0$ . *This root is identified as the GL mode in this study.* Among the two remaining roots obtained from the  $\text{Re}=0$  analysis, one root is highly stable at low  $k$  and when continued to finite  $k$ , it is found that this mode becomes unstable when the solid layer becomes sufficiently soft, i.e., beyond a critical  $\Gamma$ . This finite- $k$  behavior is typical of the unstable mode predicted first by Kumaran *et al.*<sup>26</sup> *This root is identified as the LS interfacial mode.* The third root from the  $\text{Re}=0$  analysis was never observed to have a positive growth rate for a wide range of parameters. Each of these roots are found analytically from the  $\text{Re}=0$  analysis at low values of  $k$  and are continued to arbitrary  $k$  using a numerical procedure similar to one used in Refs. 11 and 12.

For the neo-Hookean model, the differential equation in the solid is integrated numerically,<sup>16</sup> and the characteristic equation is again cubic in  $c$  and has three roots. It is shown in Sec. III C below that, in the limit of low  $k$ , the contribution due to additional couplings between base flow and fluctuations present in the neo-Hookean model [the terms under-

lined in Eqs. (10)–(12) and Eq. (22)] become subdominant and the governing stability equations in the low- $k$  limit are identical for the linear elastic solid and neo-Hookean models. Thus, the low- $k$  asymptotic results obtained for the linear elastic model<sup>12</sup> will be unaffected by the use of the neo-Hookean model. Hence, at small  $k$ , one of the three roots from the  $\text{Re}=0$  analysis for the neo-Hookean model should approach the low- $k$  GL solution obtained using linear elastic solid, and this solution is designated as the GL mode for the neo-Hookean case. However, in the discussion to follow, we will also refer to this solution as “root 1” because of a type of “mode mixing” phenomenon to be demonstrated below. As in the case of linear elastic solid, one of the remaining two roots qualitatively behaves similar to the LS instability.<sup>26</sup> This root is identified as the LS mode and will also be referred to as “root 2” in the following discussion. The third root never has a positive imaginary part for a wide range of parameters, and hence is not of interest in this discussion. By way of verification of our numerical procedure and code, we reproduced the data given in Fig. 4 of Gkanis and Kumar<sup>16</sup> using our numerical procedure for both linear-elastic and neo-Hookean solids.

#### B. Results in the zero-Re limit

At  $\text{Re}=0$ , there is no GL mode instability for liquid flow down a rigid inclined plane.<sup>1,12</sup> Instabilities, if any, present at  $\text{Re}=0$  for an inclined plane coated with a solid layer must then be due to the deformability of the solid layer. It is useful here to call  $\Gamma = \mu V/ER$  as the “solid deformability parameter,” since  $\Gamma \rightarrow 0$  represents the rigid wall limit (of infinite shear modulus  $E$ ), and an increase in  $\Gamma$  makes the solid layer more deformable. Recently, Gkanis and Kumar<sup>16</sup> used both linear elastic and neo-Hookean models to study the present problem in the creeping-flow limit, and reported that only the LS mode gets destabilized by wall deformability while the other interfacial mode remains unaffected by the soft solid layer. The same configuration was considered by Shankar and Sahu<sup>12</sup> but with linear viscoelastic solid, who showed that both GL and LS modes can become unstable due to solid deformability at nonzero  $\text{Re}$  and finite  $k$ . In view of these apparently contradicting results, we re-examine below the effect of solid layer deformability on both the interfacial modes using both the solid models at  $\text{Re}=0$ .

##### 1. Linear elastic solid

Figure 1 shows the neutral curves in the  $\Gamma$ - $k$  plane for both GL and LS modes at different values of solid layer thickness. In order to compare our results with those of Gkanis and Kumar,<sup>16</sup> the definition of parameters in Fig. 1 is same as in Fig. 2 of Ref. 16. The nondimensional parameters in the present study are related to the ones used in Ref. 16 as

$$\Gamma = G \frac{\sin \theta}{2},$$

$$T_1 = \Gamma \Sigma, \quad T = \Gamma \Sigma_1$$

where  $G$  is the deformability parameter and  $T$  and  $T_1$  are the interfacial tension parameters at LS and GL interfaces, re-

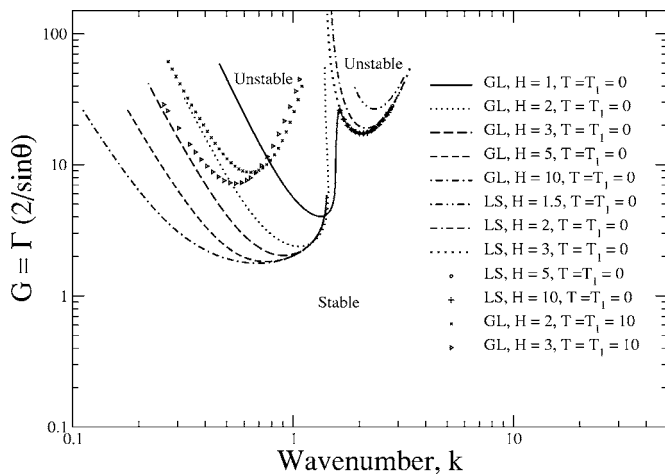


FIG. 1. Neutral stability curves for both GL and LS modes for the linear elastic solid in terms of Gkanis and Kumar's (Ref. 16) parameters:  $Re=0$ ,  $\theta=50^\circ$ .

spectively, as defined in Ref. 16. When  $T=T_1=0$ , Fig. 1 demonstrates that both the interfaces become unstable as  $\Gamma$  (or equivalently  $G$ ) is increased beyond a critical value. The critical value of  $\Gamma$  required to destabilize each mode is given by the minimum of the respective neutral curves and the corresponding wave number is identified as the critical wave number. The two unstable regions (corresponding to GL and LS modes) exist at different bands of wave numbers. Figure 1 also shows that as  $H$  is increased, the critical  $\Gamma$  and wave number (for both GL and LS modes) become independent of  $H$  and approach a constant value. This is in agreement with the result reported (for what was referred to as the "LS" mode) by Gkanis and Kumar.<sup>16</sup> However, they concluded that only the LS mode can become unstable while the GL mode remains stable in the presence of the deformable solid layer. Using our numerical procedure, we reproduced the results given by Gkanis and Kumar<sup>16</sup> for the linear elastic solid (Fig. 2 of their paper) and found that those results in fact correspond to the continuation of the low- $k$  GL mode to finite  $k$  and  $\Gamma$ .

To make this clarification transparent, we present neutral curves for two different values of  $H=2$  and 3 (see Fig. 1) with the same set of parameters as in Fig. 2 of Gkanis and Kumar (i.e., with  $T=T_1=10$ ). The critical conditions obtained from Fig. 1 for the GL mode neutral curves agrees very well with the critical  $G$  given in Fig. 2 of Gkanis and Kumar for  $H=2$  and 3. Excellent agreement was also found for other values of solid thicknesses. *However, this unstable mode was identified as the LS mode in Ref. 16.* We, by contrast, obtained the same results by continuation of the low- $k$  GL mode asymptotic solution. Moreover, we found that for the high values of interfacial tension parameter ( $T=T_1=10$ ) used by Gkanis and Kumar,<sup>16</sup> no instability was present for LS mode even at very large values of  $\Gamma$ . The nondimensional group  $T=\gamma_1/(ER)$  can be estimated using  $\gamma_1\sim 0.1$  N/m (already on the higher side),  $E\sim 10^4$  Pa, which implies  $T=10^{-5}/R$  where  $R$  is in meters. In order for  $T$  to be 10, we therefore require  $R$  to be  $O(10^{-6})$  m, which corresponds to extremely thin liquid films. If one considers liquid films of

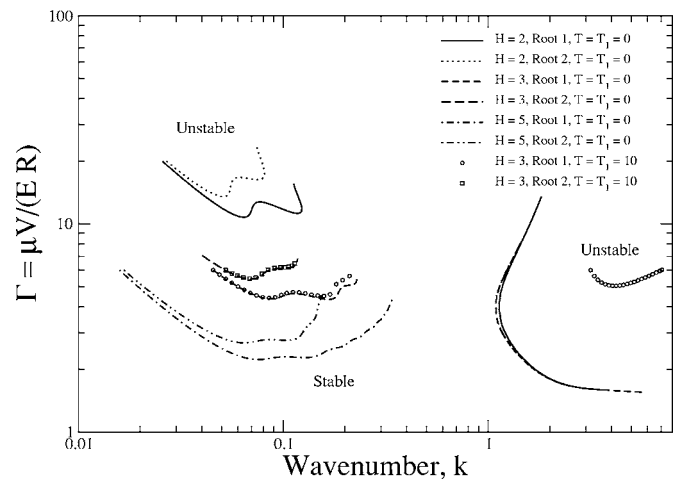


FIG. 2. Neutral curves for GL and LS modes for different  $H$  in the neo-Hookean solid:  $\Gamma$  vs  $k$  for  $Re=0$ ,  $\theta=50^\circ$ , for two different values of interfacial tension parameter  $T$ .

thickness of  $O(10^{-3})$  m and shear modulus  $E\sim 10^4$  Pa, then  $T\sim 10$  corresponds to unusually large interfacial tensions of  $O(100)$  N/m. Therefore, for realistic values of interfacial tension, shear modulus, and fluid thickness,  $T$  cannot be as high as 10. When  $T=T_1=0$ , it has already been shown that both the interfaces can become unstable as the deformability of the solid is increased beyond a critical value. We have further verified that for realistic values of interfacial tension parameters  $\Sigma\sim\Sigma_1\sim 0.01$  (results not displayed), there is no effect of interfacial tension on GL mode neutral curves, while interfacial tension has a stabilizing effect on LS mode neutral curves. Thus, the results presented in this study confirm that for the linear elastic solid, there are indeed two unstable modes present in the system, namely GL and LS modes, which can become unstable at  $Re=0$  and finite  $k$  as solid deformability  $\Gamma$  is increased.

## 2. Neo-Hookean solid

Even in the case of neo-Hookean solid, Gkanis and Kumar<sup>16</sup> identified the unstable mode as the LS mode, suggesting that the GL mode remains stable due to wall deformability. We address here the question of whether two different unstable modes exist at finite  $k$  due to the presence of a deformable wall in the neo-Hookean case. Recall that at  $Re=0$ , the characteristic equation was cubic in  $c$  and has three roots. Among the three roots, root 1 and root 2 correspond, respectively, to GL and LS modes, in the low- $k$  limit (refer to Sec. III A for details of mode identification).

Figure 2 presents the neutral curves for both root 1 and root 2 for different values of solid thickness and for both zero and nonzero interfacial tensions. For a given value of solid thickness and interfacial tensions, there are three different branches of neutral curves: two corresponding to root 1 and one corresponding to root 2. Recall that root 1 corresponds to the GL mode in the low- $k$  limit, so it seems reasonable to refer to root 1 neutral curves as GL mode neutral curves. The neutral curves for root 1 show that for  $\Gamma$  greater than a critical value, root 1 remains stable at low wave numbers, but becomes unstable for an intermediate range of  $k$ . It

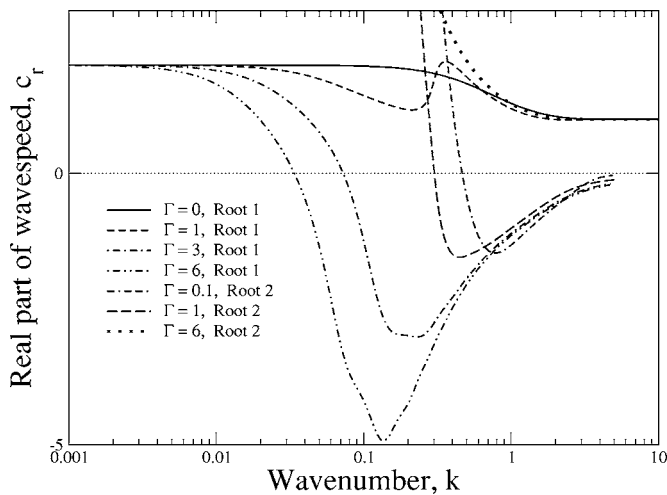


FIG. 3. Results showing mode exchange between root 1 and root 2 in the neo-Hookean solid:  $c_r$  vs  $k$  for  $\text{Re}=0$ ,  $H=3$ ,  $\theta=50^\circ$ ,  $\Sigma=\Sigma_1=0$ .

again becomes unstable at higher values of  $k$ . This high- $k$  instability was never observed for the linear elastic solid upon continuation of the GL mode. We discuss the nature of this high- $k$  instability a little later. Root 2 neutral curves, which correspond to the LS mode, also show instability at finite wave numbers as  $\Gamma$  is increased beyond a particular value. These neutral curves clearly indicate that even for the neo-Hookean model, both roots 1 and 2 (corresponding to GL and LS modes) can become unstable at finite  $k$  due to wall deformability at zero  $\text{Re}$ . This conclusion is different from the one reached by Gkanis and Kumar.<sup>16</sup>

While generating  $c$  vs  $k$  data for different  $H$  and  $\Gamma$ , we observed a type of mode “switching” phenomenon between root 1 and root 2, at finite  $\Gamma$  and  $k$ . Interfacial modes are usually labeled on the basis of their asymptotic behavior in low and high  $k$  limit. For instance, the imaginary part of root 1 (which is obtained from the low  $k$  results for the GL mode) has  $c_i \rightarrow 0$  as  $k \rightarrow 0$ , while the real part,  $c_r$ , approaches the leading order wavespeed for liquid flow down a rigid inclined plane as  $k \rightarrow 0$ .<sup>1,12</sup> Also, in the limit of high  $k$ , root 1 in the presence of a soft solid layer matches with the free-surface GL mode eigenvalue for liquid flow down a rigid inclined plane. This is because, at high  $k$ , the fluid velocity fluctuations are localized near the respective interfaces, and the deformability of the solid layer is expected to have negligible effect on the GL mode at high  $k$ . We observed this expected trend for root 1 in the presence of the solid layer when  $\Gamma$  is low. However, beyond a particular value of  $\Gamma$ , root 1, which coincides with the GL mode solution in the low- $k$  limit, when continued to higher  $k$ , changes its behavior and does not approach the GL mode curve for rigid wall at high  $k$ . Instead, it is root 2 (which is obtained by continuing the LS mode at low- $k$ ) that approaches the high- $k$  GL-mode behavior. This suggests that the low- $k$  and high- $k$  behavior of the two roots (1 and 2) gets interchanged beyond a critical  $\Gamma$  at finite values of  $k$ . This exchange is clearly demonstrated in the  $c_r$ - $k$  plane shown in Fig. 3 for different values of  $\Gamma$  and at  $H=3$ . The solid line presents the data for rigid inclined plane ( $\Gamma=0$ ). When  $\Gamma$  is increased to 1 there is no mode

exchange between the two roots, and both the roots exhibit expected behavior at low- $k$  and high- $k$  limits, e.g., at low  $k$  and high  $k$ ,  $c_r$  for root 1 approaches the GL mode behavior in rigid channels with  $\Gamma=0$ . However, when  $\Gamma$  is further increased to 3 and 6, the  $c_r$  values for root 1, at sufficiently high  $k$ , exhibits behavior similar to the LS mode in the limit of high  $k$ . Similarly, for  $\Gamma=6$ , the wavespeed for root 2 matches with the high- $k$  behavior of the GL mode in rigid surfaces. This discussion indicates that, at high enough  $\Gamma$  the same root exhibits GL mode behavior at low  $k$ , but has the characteristics of the LS mode at higher wave numbers and vice versa. A similar phenomenon was earlier reported for the two-layer viscoelastic plane Couette flow past a deformable solid layer by Shankar.<sup>13</sup> Mode exchange and mode mixing phenomena as well as resonance have been extensively discussed in the literature in other contexts as well, such as in two-layer Benard-Marangoni instability.<sup>31,32</sup> In light of the exchange in the behavior of the two modes at higher values of  $\Gamma$ , the designation of the two modes as GL and LS depends on whether the low- $k$  or high- $k$  behavior is used for labeling. In this work, we use the nomenclature based on low- $k$  asymptotic behavior of the two roots to classify them as GL and LS.

With this picture, it is now possible to understand the high- $k$  instability of root 1 (nominally the GL mode) demonstrated in Fig. 2. Because there is mode switching between root 1 and root 2 at finite  $k$  and  $\Gamma$ , the high- $k$  instability observed for root 1 is in fact the high- $k$  instability of the LS mode,<sup>16,27</sup> as the two roots had already switched at some finite  $k$ . Thus, the root 1 neutral curves at high wave numbers represent the short wave LS mode instability due to first normal stress difference in the base state (reported by Gkanis and Kumar<sup>16</sup>). On the other hand, root 1 and 2 neutral curves at finite wave numbers correspond, respectively, to GL and LS mode instabilities due to wall deformability. Note that for the neo-Hookean solid, both GL and LS modes are unstable in similar range of finite wave numbers, unlike the linear elastic model where the two unstable modes exist for two different ranges of wave numbers. In addition, the critical  $\Gamma$  as well as critical wave number decreases with an increase in  $H$  for GL and LS mode instability, in contrast to the linear elastic solid.<sup>16</sup> Thus, there are qualitative differences between the neutral curves obtained from the two different solid models for the finite- $k$  instabilities. Nevertheless, the critical  $\Gamma$  for the GL mode is lower than that for the LS mode, similar to the results for the linear elastic solid. The neutral curves pertaining to high-wave number instability of the LS mode, though, remain largely independent of  $H$ , as would be expected for short-wavelength fluctuations.

In Fig. 2, we also illustrate the role of interfacial tension at both the interfaces on the neutral curves corresponding to different modes for  $H=3$ . In order to emphasize the (lack of) role of interfacial tension, we choose a very high value of the nondimensional parameter  $T=10$  used in Ref. 16 at both the GL and LS interfaces. Nevertheless, Fig. 2 shows that even this high value of interfacial tension at both the interfaces has very little effect on the finite- $k$  neutral curves for the LS and GL modes. As expected, and as was shown in the earlier works of Gkanis and Kumar, the high- $k$  instability in the

neo-Hookean solid due to the normal stress difference is significantly stabilized by the interfacial tension at the LS interface. This lack of effect of interfacial tension on the finite- $k$  neutral curves for the neo-Hookean solid is in stark contrast to the results obtained earlier for the linear elastic solid, where we showed that the LS neutral curve disappears for very high values of the nondimensional parameter  $T=10$ .

Thus, we have shown that even in the creeping-flow limit, there are indeed two modes of instability (corresponding to GL and LS interfaces) which get excited as the solid layer deformability is increased, and this conclusion holds for both neo-Hookean as well as the linear elastic solid.

### C. Results at finite Re

In the presence of inertia, the free-surface (GL) mode could become unstable in flow down a rigid incline at low wave number. Shankar and Sahu<sup>12</sup> used the linear elastic model and showed that the GL instability in rigid inclines can be suppressed by deformability of the solid layer. However, as pointed out by Gkanis and Kumar<sup>16</sup> (also see the foregoing discussion), there are qualitative differences in the results from the linear elastic and nonlinear neo-Hookean solid at  $Re=0$ , particularly in the variation of critical conditions (for finite- $k$  instability at higher values of  $\Gamma$ ) with solid thickness. Thus, we first investigate the effect of inertia on the dependence of critical conditions on  $H$  for the finite- $k$  instabilities in the system. We then examine whether the suppression of instability predicted<sup>12</sup> using the linear elastic solid exists for the neo-Hookean solid as well. Finally we present the comparison between the results obtained using the two models.

#### 1. Inertial effects on finite- $k$ instabilities

Figure 4 shows the GL and LS mode neutral curves for different values of  $H$  at  $Re=1.5$ , for the linear elastic solid. This shows that the destabilization of the two modes at finite  $k$  due to wall deformability continues to finite  $Re$ . Figure 4(a) shows that the inclusion of inertia changes the nature of GL mode neutral curves in terms of variation of critical conditions with  $H$ . The critical  $\Gamma$  as well as wave number decrease as the solid layer thickness is increased, in contrast to the results (see Fig. 1) in the creeping flow limit.<sup>16</sup> Similar behavior is observed for the LS mode [see Fig. 4(b)] at finite  $Re$ . Figure 5(a) and 5(b), respectively, show the GL and LS mode neutral curves at finite- $k$ , for  $Re \neq 0$ , for the neo-Hookean solid. As with  $Re=0$ , even at finite inertia, the critical  $\Gamma$  for both modes show similar qualitative  $H$  dependence, i.e., it decreases with an increase in  $H$ . One feature worth pointing out about the GL mode neutral curves at finite  $Re$  [Fig. 5(a)] is that there are no separate branches for high- $k$  first normal stress difference driven instability and finite- $k$  GL mode instability (compare with Fig. 2 for  $Re=0$ ). We have verified that the two neutral curve branches at  $Re=0$ , i.e., one for the GL mode that exists at relatively lower but finite values of  $k$  and the other that corresponds to the LS mode high  $k$  instability, merge with each other beyond a particular  $Re$  around 0.05. Figure 5(a) also shows the effect of increasing the interfacial tension parameter on GL mode

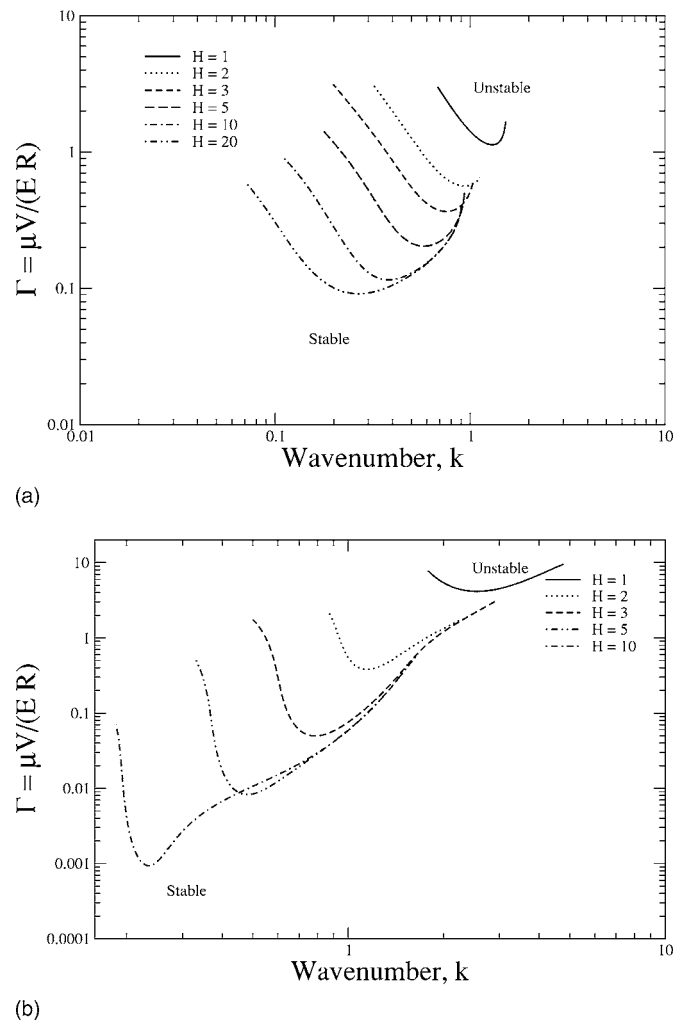
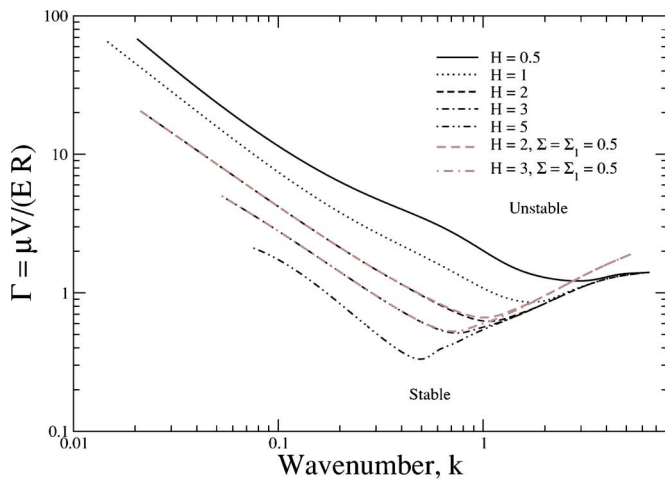


FIG. 4. Neutral stability diagrams for GL and LS modes for the linear elastic solid at finite inertia: Data for  $Re=1.5$ ,  $\Sigma=\Sigma_1=0$  and  $\theta=50^\circ$ . (a)  $\Gamma$  vs  $k$ : GL mode. (b)  $\Gamma$  vs  $k$ : LS mode.

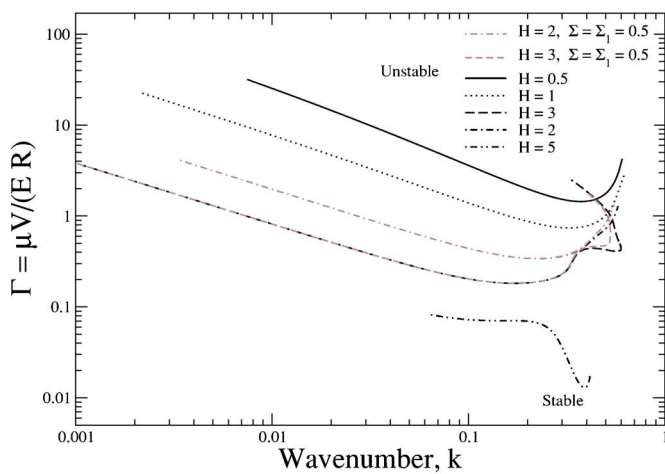
neutral curves. This figure depicts the GL mode neutral stability data for  $H=2$  and 3 with  $\Sigma=\Sigma_1=0.5$  in addition to data for  $H=0.5-5$  with  $\Sigma=\Sigma_1=0$ . This indicates that the increase in interfacial tension has some stabilizing effect for  $k > 1$ , while for  $k < 1$  the neutral curves with and without surface tension are quite similar. We also found that GL mode neutral curves remain unaffected when interfacial tension parameter (both  $\Sigma$  and  $\Sigma_1$ ) is increased to reasonable values [of the  $O(0.01)$ ]. Figure 5(a) also shows that in the limit of high  $k$ , and for a given interfacial tension, the neutral curves become  $H$  independent. This is expected, as the short-wave perturbations are localized near the respective interfaces, and hence will not be affected by the thickness  $H$  of the solid layer. Figure 5(b) shows that increasing interfacial tension to high values does not alter the LS mode neutral curves significantly except for a slight stabilization for  $k > 0.4$ .

#### 2. Suppression of GL mode instability

Hitherto, we discussed results where the deformability of the solid layer induced instability at finite  $k$  in both solid models. We now address the question of whether the stabilization of the low- $k$  GL mode instability predicted using the



(a)



(b)

FIG. 5. Neutral stability diagrams for GL and LS modes for a neo-Hookean solid at finite inertia. Data for  $Re=1.5$ ,  $\Sigma=\Sigma_1=0$ , and  $\theta=50^\circ$ . (a)  $\Gamma$  vs  $k$ : GL mode. (b)  $\Gamma$  vs  $k$ : LS mode.

linear viscoelastic model<sup>12</sup> holds for the neo-Hookean model as well. We start by investigating the problem in the limit of low wave number. It was noted in Sec. II that there are additional terms in the linearized equations [underlined terms in Eqs. (10)–(12) and Eq. (22)] for the neo-Hookean solid, which are absent for the linear elastic model. We have verified by performing a long wave analysis<sup>12</sup> that these additional terms remain subdominant in the limit of low  $k$ , and hence the results from the long wave analysis for the linear elastic solid hold exactly for the neo-Hookean model as well. This can be illustrated with the help of the low  $k$  scalings of various physical quantities:<sup>12</sup> at low  $k$ ,  $\tilde{v}_z \sim O(1)$ ,  $\tilde{v}_x \sim O(1/k)$ ,  $\tilde{p} \sim O(1/k^2)$  and  $\tilde{w}_z \sim O(1)$ ,  $\tilde{w}_x \sim O(1/k)$ ,  $\tilde{p}_s \sim O(1/k^2)$ . It can be seen from Eq. (10) that the coupling term,  $(2\Gamma X_3)ik\tilde{w}_z$ , is  $O(k)$  smaller compared to other terms in the equation. The additional underlined term present in the  $x$  momentum equation (11) is  $O(k^2)$  smaller compared to other terms present in the equation. Similarly it can be verified in the remaining governing equation and tangential stress balance at the LS interface that the coupling terms arising due to constitutive nonlinearities in the neo-Hookean solid are (at

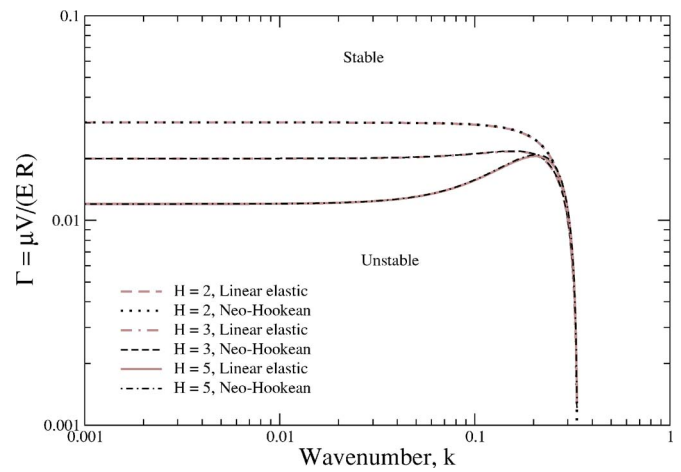


FIG. 6. Comparison of results from linear elastic and neo-Hookean solid showing stabilization of low  $k$  GL mode instability as  $\Gamma$  is increased from zero:  $\Gamma$  vs  $k$  for  $Re=1.5$ ,  $\theta=50^\circ$ ,  $\Sigma=\Sigma_1=0$ .

least)  $O(k)$  smaller than other terms. Hence, the previous low  $k$  results of Shankar and Sahu<sup>12</sup> for the linear elastic solid carry over exactly for the neo-Hookean solid as well. It was shown in Ref. 12 that the system is neutrally stable at leading order, and the stability is determined by the  $O(k)$  correction to wavespeed. The leading order and first correction to wavespeed are given as<sup>12</sup>

$$c^{(0)} = 2, \quad (24)$$

$$c^{(1)} = i \left[ \left( \frac{4}{5} Re - \frac{2}{3} \cot \theta \right) - 6\Gamma H \right]. \quad (25)$$

The term proportional to  $\Gamma H$  represents the effect of solid layer deformability on the free-surface instability. When  $\Gamma \rightarrow 0$  or  $H=0$ , one obtains the limit of a rigid incline, and in this limit, the above result reduces to the classical result of Yih.<sup>1</sup> When  $\Gamma \neq 0$  and  $H \neq 0$ , the above result shows that the solid layer has a stabilizing effect on the free-surface instability in a rigid incline. For reasons outlined above, these results for  $c^{(0)}$  and  $c^{(1)}$  will also hold for the neo-Hookean solid. We have explicitly verified this using the results from our full numerical code for the neo-Hookean solid, which agreed very well with the above low  $k$  asymptotic result obtained using the linear viscoelastic solid. Hence, for long waves, the effect of solid layer remains stabilizing even for the neo-Hookean model. These results at low  $k$  can be continued to arbitrary  $k$  in order to determine the neutral stability conditions in the  $\Gamma$ – $k$  plane. Figure 6 shows the neutral stability curves for both neo-Hookean and linear elastic solid when the results are continued from low  $k$  to finite wave numbers. This figure provides the values of the parameter  $\Gamma$  above which there is a transition from unstable GL mode perturbations to stable GL perturbations for  $Re=1.5$  and at different  $H$ . This figure clearly illustrates that *the neutral curves remain identical for both solid models even at finite  $k$* . Further, the critical  $\Gamma$  above which instability suppression is realized is  $O(0.01)$  where the linear elastic model is expected to be accurate, and the difference between two solid models arise only for much higher values of  $\Gamma$ . Thus, it is clear that

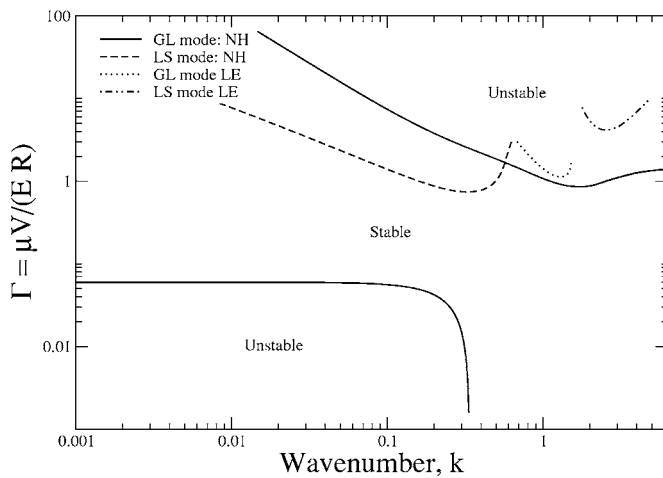


FIG. 7. Comparison between results from linear elastic and neo-Hookean models. Neutral curves for GL and LS modes:  $\Gamma$  vs  $k$  for  $H=1$ ,  $Re=1.5$ ,  $\theta=50^\circ$ ,  $\Sigma=\Sigma_1=0$ .

the use of neo-Hookean model does not have any effect on the prediction of instability suppression obtained using the linear elastic model.

However, to complete the picture, we must plot the “upper” neutral curves which represent the finite  $k$  destabilization of the GL and LS modes due to wall deformability. These upper neutral curves differ significantly for two solid models. Thus it is pertinent to ask whether the difference in these curves affects the existence of the stability window for the neo-Hookean solid. Figure 7 presents a typical neutral stability plot for both solid models with  $H=1$ ,  $Re=1.5$ ,  $\Sigma=\Sigma_1=0$ . The lower GL mode neutral curves, which denote the transition from unstable to stable GL mode perturbations, remain exactly identical for both models. With further increase in  $\Gamma$ , the flow could again become unstable due to the excitation of LS or GL mode at higher wall deformability. Importantly, even for the neo-Hookean model, there exists a window of stability (in the parameter  $\Gamma$ ) where all the unstable modes are suppressed. Figure 8 shows that a similar picture of instability suppression holds for a vertical incline

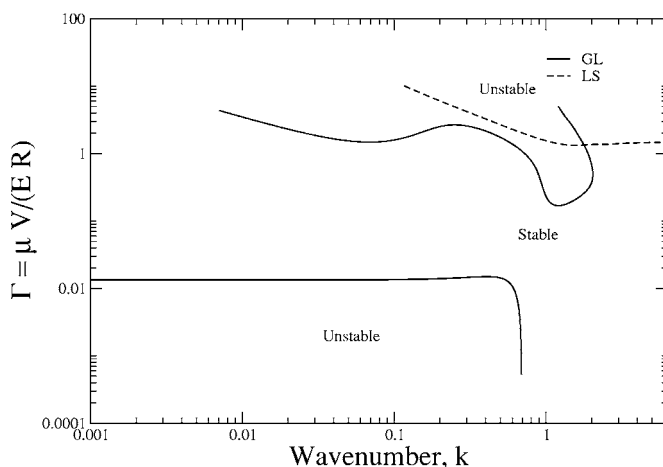


FIG. 8. Neutral stability curves illustrating instability suppression in the neo-Hookean solid for the vertical geometry:  $\Gamma$  vs  $k$  for  $H=1.0$ ,  $Re=0.1$ ,  $\theta=90^\circ$ ,  $\Sigma=\Sigma_1=0.1$ .

( $\theta=90^\circ$ ) as well. Thus, the qualitative conclusion that a deformable solid layer can be used to obtain a stable flow configuration, which was otherwise unstable in a rigid inclined plane, remains independent of the solid model used. Of course, the upper neutral curves differ in detail for both solid models, and will be predicted more accurately by the neo-Hookean model. For example in Fig. 7, on comparing the GL mode upper neutral curves for both the solid models, one can see that the band of unstable wave numbers for the neo-Hookean solid is quite large as compared to the GL mode upper neutral curve for the linear elastic solid. Similar inference can be made for the LS mode. We also found that as the thickness of the solid layer is decreased, the gap between upper and lower neutral curves is increased indicating an increased window in  $\Gamma$  for which flow remains stable. On the other hand, the stability window vanishes at higher values of solid thicknesses. In all, these results demonstrate that it is indeed possible to obtain a stable flow regime by tuning the solid layer parameters ( $H$  and  $\Gamma$ ). The use of a more complex neo-Hookean model does not alter the predicted stabilization obtained from the linear elastic model.

#### IV. CONCLUSIONS

The stability of gravity-driven free-surface flow down an inclined plane lined with a deformable solid is analyzed in order to examine the effect of solid deformability on the free-surface instability, and to compare and contrast the results obtained from two different constitutive relations for the solid, viz., linear elastic and neo-Hookean. In addition to the free-surface (GL) mode of instability, the interfacial mode corresponding to the liquid-solid (LS) interface could also become unstable in the present system. In the creeping-flow limit, where the GL instability is absent in a rigid incline, we show for both the solid models that the solid deformability destabilizes both the GL and LS modes at finite wave numbers. This conclusion differs from the analysis of Gkanis and Kumar<sup>16</sup> who predicted only one unstable mode, which we show to be the continuation of the low  $k$  GL mode, and not the LS mode. For the neo-Hookean solid, there is in addition another high-wave number instability<sup>16</sup> due to the jump in the first normal stress difference in the base state. The neutral curves obtained for the finite  $k$  GL and LS instabilities from both the models differ significantly in detail. We also demonstrated a type of mode exchange between the two modes for the neo-Hookean solid, wherein the low  $k$  and high  $k$  behavior of the two interfacial modes gets interchanged as the solid layer becomes sufficiently deformable. While interfacial tension has a stabilizing effect on the LS neutral curve and little effect on the GL neutral curve for the linear elastic solid, it is shown to have a negligible effect on both the GL and LS neutral curves for the neo-Hookean solid.

At finite inertia, the GL mode instability<sup>1</sup> becomes operative in liquid flow down an inclined plane. In the presence of the deformable solid layer, we have shown that this instability can be suppressed at all wave numbers when the solid becomes sufficiently deformable, and this conclusion holds true for both neo-Hookean and linear elastic models. Indeed,

the neutral curves associated with this instability suppression are shown to be identical for both the solid models. Even at finite inertia, as the solid layer becomes more deformable, both the GL and LS modes are destabilized at finite  $k$ . The neutral curves for these unstable modes are qualitatively different for the two solid models. For both the solid models, there is a significant window in the parameter  $\Gamma$  (or equivalently, the shear modulus of the solid) where both the GL and LS modes are stabilized at all wave numbers. This stable window, however, decreases with an increase in the solid layer thickness in both models. In conclusion, the present study has employed the more rigorous neo-Hookean model and has demonstrated that free-surface instabilities can be completely suppressed by soft solid layer coatings.

- <sup>1</sup>C.-S. Yih, "Stability of liquid flow down an inclined plane," *Phys. Fluids* **6**, 321 (1963).
- <sup>2</sup>C.-S. Yih, "Instability due to viscosity stratification," *J. Fluid Mech.* **27**, 337 (1967).
- <sup>3</sup>T. B. Benjamin, "Wave formation in laminar flow down an inclined plane," *J. Fluid Mech.* **2**, 554 (1957).
- <sup>4</sup>V. Y. Shkadov, "Wave modes in the flow of thin layer of a viscous liquid under the action of gravity," *Izv. Akad. Nauk SSSR, Mekh. Zhidk. Gaza* **1**, 43 (1967).
- <sup>5</sup>Y. Renardy, "Stability of the interface in two-layer Couette flow of upper convected Maxwell liquids," *J. Non-Newtonian Fluid Mech.* **28**, 99 (1988).
- <sup>6</sup>K. P. Chen, "Elastic instability of the interface in Couette flow of two viscoelastic liquids," *J. Non-Newtonian Fluid Mech.* **40**, 261 (1991).
- <sup>7</sup>S. P. Lin, J. N. Chen, and D. R. Woods, "Suppression of instability in a liquid film flow," *Phys. Fluids* **8**, 3247 (1996).
- <sup>8</sup>W. Y. Jiang and S. P. Lin, "Enhancement or suppression of instability in a two-layered liquid film flow," *Phys. Fluids* **17**, 054105 (2005).
- <sup>9</sup>V. Y. Shkadov, M. G. Velarde, and V. P. Shkadova, "Falling films and the Marangoni effect," *Phys. Rev. E* **69**, 056310 (2004).
- <sup>10</sup>E. A. Demekhin, S. Kalliadasis, and M. G. Velarde, "Suppressing falling film instabilities by Marangoni forces," *Phys. Fluids* **18**, 042111 (2006).
- <sup>11</sup>V. Shankar and L. Kumar, "Stability of two-layer Newtonian plane Couette flow past a deformable solid layer," *Phys. Fluids* **16**, 4426 (2004).
- <sup>12</sup>V. Shankar and A. K. Sahu, "Suppression of instability in liquid flow down an inclined plane by a deformable solid layer," *Phys. Rev. E* **73**, 016301 (2006).
- <sup>13</sup>V. Shankar, "Stability of two-layer viscoelastic plane Couette flow past a deformable solid layer," *J. Non-Newtonian Fluid Mech.* **117**, 163 (2004).
- <sup>14</sup>V. Shankar, "Stability of two-layer viscoelastic plane Couette flow past a deformable solid layer: Implications of fluid viscosity stratification," *J. Non-Newtonian Fluid Mech.* **125**, 143 (2005).
- <sup>15</sup>L. E. Malvern, *Introduction to the Mechanics of a Continuous Medium* (Prentice-Hall, Englewood Cliffs, 1969).
- <sup>16</sup>V. Gkanis and S. Kumar, "Instability of gravity-driven free-surface flow past a deformable elastic solid," *Phys. Fluids* **18**, 044103 (2006).
- <sup>17</sup>C. Macosko, *Rheology: Principles, Measurements, and Applications* (VCH, New York, 1994).
- <sup>18</sup>G. A. Holzapfel, *Nonlinear Solid Mechanics* (Wiley, Chichester, 2000).
- <sup>19</sup>H.-C. Chang and E. A. Demekhin, *Complex Wave Dynamics on Thin Films* (Elsevier, Amsterdam, 2002).
- <sup>20</sup>A. A. Nepomnyashchy, M. G. Velarde, and P. Colinet, *Interfacial Phenomena and Convection* (Chapman and Hall/CRC, London, 2001).
- <sup>21</sup>J. M. Floryan, S. H. Davis, and R. E. Kelly, "Instabilities of a liquid film down a slightly inclined plane," *Phys. Fluids* **30**, 983 (1987).
- <sup>22</sup>T. W. Kao, "Role of viscosity stratification in the instability of two-layer flow down an incline," *J. Fluid Mech.* **33**, 561 (1968).
- <sup>23</sup>D. S. Loewenherz and C. J. Lawrence, "The effect of viscosity stratification on the stability of a free surface flow at low Reynolds number," *Phys. Fluids A* **1**, 1686 (1989).
- <sup>24</sup>K. P. Chen, "Wave formation in the gravity-driven low-Reynolds number flow of two liquid films down an inclined plane," *Phys. Fluids A* **5**, 3038 (1993).
- <sup>25</sup>W. Y. Jiang, B. Helenbrook, and S. P. Lin, "Inertialess instability of a two-layer liquid film flow," *Phys. Fluids* **16**, 652 (2004).
- <sup>26</sup>V. Kumaran, G. H. Fredrickson, and P. Pincus, "Flow induced instability of the interface between a fluid and a gel at low Reynolds number," *J. Phys. II* **4**, 893 (1994).
- <sup>27</sup>V. Gkanis and S. Kumar, "Instability of creeping Couette flow past a neo-Hookean solid," *Phys. Fluids* **15**, 2864 (2003).
- <sup>28</sup>V. Kumaran and R. Muralikrishnan, "Spontaneous growth of fluctuations in the viscous flow of a fluid past a soft interface," *Phys. Rev. Lett.* **84**, 3310 (2000).
- <sup>29</sup>M. D. Eggert and S. Kumar, "Observations of instability, hysteresis, and oscillation in low-Reynolds number flow past polymer gels," *J. Colloid Interface Sci.* **274**, 234 (2004).
- <sup>30</sup>V. Gkanis and S. Kumar, "Stability of pressure-driven creeping flows in channels lined with a nonlinear elastic solid," *J. Fluid Mech.* **524**, 357 (2005).
- <sup>31</sup>A. Y. Rednikov, P. Colinet, M. G. Velarde, and J. C. Legros, "Two-layer Benard-Marangoni instability and the limit of transverse and longitudinal waves," *Phys. Rev. E* **57**, 2872 (1998).
- <sup>32</sup>A. Y. Rednikov, P. Colinet, M. G. Velarde, and J. C. Legros, "Rayleigh-Marangoni oscillatory instability in a horizontal liquid layer heated from above: Coupling and mode mixing of internal and surface dilatational waves," *J. Fluid Mech.* **405**, 57 (2000).